A screening method for binding synthetic metallo-complexes to haem proteins

Opdam, L.V.; Polanco Rivas, E.A.; Regt, B. de; Lambertina, N.; Bakker, C.; Bonnet, S.A.; Pandit, A.

A screening method for binding synthetic metallo-complexes to haem proteins

Laura V. Opdam [a], Ehider A. Polanco [b], Boyd de Regt [a], Nicole Lambertina [a], Cas Bakker [a], Sylvestre Bonnet [b], Anjali Pandit [a,*]

[a] SSNMR/BPOC, Einsteinweg 55, 2333 CC, Leiden, the Netherlands
[b] MCBIM Departments, Leiden Institute of Chemistry, Leiden University, Einsteinweg 55, 2333 CC, Leiden, the Netherlands

ARTICLE INFO

ABSTRACT

The introduction of a second coordination sphere, in the form of a protein scaffold, to synthetic catalysts can be beneficial for their reactivity and substrate selectivity. Here we present semi-native polyacrylamide gel electrophoresis (semi-native PAGE) as a rapid screening method for studying metal complex-protein interactions. Such a screening is generally performed using electron spray ionization mass spectrometry (ESI-MS) and/or UV–Vis spectroscopy. Semi-native PAGE analysis has the advantage that it does not rely on spectral changes of the metal complex upon protein interaction and can be applied for high-throughput screening and optimization of complex binding. In semi-native PAGE non-denatured protein samples are loaded on a gel containing sodium dodecyl sulphate (SDS), leading to separation based on differences in structural stability. Semi-native PAGE gel runs of catalyst-protein mixtures were compared to gel runs obtained with native and denaturing PAGE. ESI-MS was additionally realised to confirm protein-complex binding. The general applicability of semi-native PAGE was investigated by screening the binding of various cobalt- and ruthenium-based compounds to three types of haem proteins.

1. Introduction

There has been a surge in the design and production of artificial metalloproteins, with a wide range of functionalities, since the year 2000 [1,2]. Protein scaffolds can offer an asymmetric and tuneable chemical environment to catalytically active metal complexes, which could improve the selectivity and reactivity and provide information about their reaction mechanism [1]. Different techniques can be employed to bind a synthetic catalyst to a protein scaffold: covalent attachment to e.g. cysteine residue or to an unnatural amino acid, binding via supramolecular interactions, metal exchange and attachment via dative interaction [2]. In our present study, the focus lies on artificial metalloproteins prepared via coordination by histidine.

For screening the binding of transition metal complexes to proteins and for optimization of reaction conditions, a screening technique is desirable that can quickly and reliably identify protein-catalyst complexes requiring very little sample. Analysis of metal complex-protein interactions is typically done using electron spray ionization mass spectrometry (ESI-MS) or UV–Vis spectroscopy [3–7]. Both techniques

typically require 5–120 μg of sample per data point, which can be time consuming to obtain in the context of a larger screening, data analysis can be complex and specific equipment is required. Here we introduce a polyacrylamide gel electrophoresis (PAGE) based technique to perform a screening to identify promising protein-catalyst combinations and to optimize reaction conditions before further analysis with ESI-MS and UV–Vis is performed.

Sodium dodecyl sulphate polyacrylamide gel electrophoresis (SDS-PAGE) is fast and requires very little sample, however SDS-PAGE (ideally) separates proteins based on their mass only. SDS-PAGE involves denaturing protein samples by heating at 70–100 °C in the presence of 1) the surfactant SDS, to unfold and solubilize the protein and to provide uniform charge distributions and 2) β-mercaptoethanol, which is added to break sulphur bridges [8–10]. In an SDS-PAGE experiment protein samples are loaded on denaturing gels containing SDS. Small modifications of the molecular weight of the protein (such as those involved with the binding of small metal complexes) may not be sufficient for separation on gel. Another way to perform gel electrophoresis is by native PAGE gel analysis, in which no denaturing agents

are used. In native PAGE, the fold, oligomeric state and charge of the protein are maintained and all contribute to the speed of migration through the gel [11]. However, as we will demonstrate, when protein modifications are small in size and neutral in charge (as is the case for most of our target complexes, see below) the binding of the complex does not necessarily lead to separated bands on native gel.

In this study a new approach for screening the binding of transition-metal complexes is introduced, where semi-native gel analysis is used. A large variety of methods exist that are referred to as semi-native gel electrophoresis in literature [12–20]. We use the term to indicate that samples are prepared like for a native gel (i.e. without denaturing conditions), while the gels contain SDS as in a denaturing SDS-PAGE. We will show that semi-native PAGE can separate modified proteins containing transition-metal complexes from unbound proteins. In a two-step procedure, binding of transition metal complexes to three types of haem proteins was screened by semi-native PAGE and positive samples were subjected to ESI-MS to determine the present binding stoichiometries and detect whether axial ligands of our complexes remained after binding to the protein.

2. Material and methods

All chemicals were of analytical grade and were purchased from Sigma Aldrich unless otherwise specified. Myoglobin (Mb) from equine skeletal muscle was commercially obtained from Sigma Aldrich (M0630-1G, Missouri, USA).

2.1. Synthesis and purification of complexes

2.1.1. Synthesis of Ruthenium [2,2′:6′,2″-terpyridine]-6,6″-dicarboxylate (Ru1)

[2,2′:6′,2″-terpyridine]-6,6″-dicarboxylic acid (compound I) was synthetized following the procedure described in Galaup et al. 2005 [21], modified as follows: [Terpyridine]-6,6′-dicarbonitrile (1.5 g, 5.29 mmol), ethanol (100 mL) and water (20 mL) were mixed in a 250 mL round-bottom flask. KOH (2.8 g, 49.9 mmol) was added to the mixture. The reaction mixture was refluxed overnight. TLC performed in Hexane/EtOAc (9:1) showed consumption of starting materials. Then the solvent was evapored and the resulting white residue was dissolved in water (100 mL). Upon adjusting the pH to 4 with aqueous HCl (1 M), a white precipitate was observed. The precipitate was removed by filtration and washed with cold water (2×50 mL) and acetonitrile (2×50 mL). Afterward, the solid was heated to reflux in a mixture of concentrated H_2SO_4/concentrated CH_3COOH (100 mL, 1:1) for 5 h. The reaction mixture was then poured onto ice. A white solid precipitate was formed and was filtered and washed with cold water and acetonitrile. The white solid was left to dry overnight under vacuum. (Yield: 70%) ^{1}H NMR: (400 MHz, DMSO) δ 13.34 (s, 1H), 8.88 (dd, $J = 7.8$, 1.3 Hz, 1H), 8.66 (d, $J = 7.8$ Hz, 1H), 8.22 (t, $J = 7.8$ Hz, 1H), 8.16 (dd, $J = 7.6$, 1.2 Hz, 1H). Ruthenium [2,2′:6′,2″-terpyridine]-6,6″-dicarboxylate (DMSO) (H_2O) (**Ru1**) was synthetized following the procedure described by Matheu et al. 2018 [22].

2.1.2. Synthesis of Ruthenium(1,2-bis(pyridine-2-carboxamido)-4,5-dimethylbenzene (2-)(CO)(OH₂) (Ru2)

N,N'-(1,2-phenylene)dipicolinamide (compound II) was synthetized following the procedure described by Kärkäs et al. 2013 [23]. Ruthenium(N,N'-(1,2-phenylene)dipicolinamide)(CO)(H₂O) (**Ru2**) was synthetized following the procedure described by Kärkäs et al. 2013 [23], modified as follows: $RuCl_3 \cdot nH_2O$ (150 mg, 0.471 mmol) was added to a solution of N,N'-(1,2-phenylene)dipicolinamide (150 mg, 0.471 mmol)) (compound II) and sodium hydride (22.56 mg, 0.94 mmol) in dry DMF (4 mL) under constant stirring. The reaction mixture was refluxed under nitrogen overnight after which the solvent was evaporated under reduced pressure. MeCN (10 mL) was added to the residue and the black precipitate was filtered off. After the addition of H₂O, the mixture was

kept in the fridge overnight to afford a dark-green precipitate. Filtering and washing with H₂O (3×20 mL) gave **Ru2** (dark-green solid). (Yield: 14%) ^{1}H NMR (400 MHz, MeOD) δ 9.01 (dd, $J = 5.3$, 0.8 Hz, 1H), 8.65 (dd, $J = 6.2$, 3.5 Hz, 2H), 8.17 (td, $J = 7.7$, 1.5 Hz, 2H), 8.09 (ddd, $J = 7.8$, 1.6, 0.7 Hz, 2H), 7.70 (ddd, $J = 7.6$, 5.2, 1.6 Hz, 2H), 7.05 (dd, $J = 6.2$, 3.5 Hz, 2H).

2.1.3. Synthesis of [Ru(II)(2,2′:6′,2″:6″,2‴-quaterpyridine)(Cl)₂] (Ru3)

(2,2′:6′,2″:6″,2‴-quaterpyridine) (Compound III) was synthetized following the procedure described by Wachter et al. 2016 [24]. [Ru(II)(2,2′:6′,2″:6″,2‴-quaterpyridine)(Cl)₂] (**Ru3**) was synthetized following the procedure described by Liu et al. 2014 [25].

2.1.4. Synthesis of [Co(II)(2,2′:6′,2″:6″,2‴-quaterpyridine)(Cl)₂]·2H₂O (Co3)

[Co(II)(2,2′:6′,2″:6″,2‴-quaterpyridine)(Cl)₂]·2H₂O (**Co3**) was synthesized following the procedure described by Leung et al. *2012* [26].

2.1.5. Synthesis of [Co(II)(2,2′:6′,2″:6″,2‴-quaterpyridine)(H₂O)₂] (ClO₄)₂ (Co4)

[Co(II)(2,2′:6′,2″:6″,2‴-quaterpyridine)(H₂O)₂] (ClO₄)₂ (**Co4**) was synthetized following the procedure described by Leung et al. *2012* [26].

2.2. Protein expression and purification

2.2.1. Expression and purification of CB5

Plasmid encoding the soluble part of bovine cytochrome B5 (CB5, kindly provided by the Ubbink lab) was transformed into the *Escherichia coli* BL21 pLysS strain, which was grown semi-anaerobically in 1.7 L Lysogeny broth (LB) medium containing 0.1 mM kanamycin and 0.1 mM chloramphenicol in a 2 L flask. Haem over expression was induced at an optical density at 600 nm (OD₆₀₀) of 0.550 using 5-aminolevulinic acid hydrochloride from Sigma Aldrich (M0630-1G, Missouri, USA). Protein expression was induced at an OD₆₀₀ of 0.6–0.8 using 1 mM Isopropyl β-D-1-thiogalactopyranoside (IPTG) at 37 °C, 140 rpm and growth was continued overnight. The pink cell pellets were obtained by 20 min centrifugation at 6k rpm, at 4 °C in a Sorval RC 6+ centrifuge from Thermo scientific (Massachusetts, USA). Cells were washed once by resuspension in 150 mM NaCl and subsequent 20 min centrifugation in an Eppendorf centrifuge (Centrifuge 5810 Eppendorf, Hamburg, Germany) at 4k rpm, 4 °C followed by resuspension in 20 mM sodium phosphate (NaPi) with 150 mM NaCl, pH 7.0. Cells were broken via sonification in a Branson Digital Sonifier (Emerson Electric Missouri, USA) set to 30%, 4 s on, 5 s off, for 7 min in an ice bath, in the presence of DNase, phenylmethylsulphonyl fluoride (PMFS) and lysozyme. Cell debris was removed via centrifugation at 11k rpm, 30 min, 4 °C (Eppendorf centrifuge 5804 R, Hamburg, Germany), followed by 30 min incubation with 0.4 M KCl and 6% w/v PEG 4000 and another round of centrifugation. Subsequently, dialysis was performed against 2 L of 20 mM NaPi pH 7.4 at 4 °C overnight using 3.5 kDa cut-off cellulose dialysis tubing from Spectrum Chemical (California, USA). Purification was performed over a DEAE column (HiTrap DEAE FF 5 mL from Sigma Aldrich, Missouri, USA) using a 300 mL gradient from 20 mM NaPi, pH 7.4–20 mM NaPi and 500 mM NaCl, pH 7.0 and red-coloured fractions were collected. This was followed by purification over a Q column (HiTrap Q HP 5 mL from Sigma Aldrich, Missouri, USA) with the same gradient. Red fractions were pooled and concentrated using 20 mL, 5.000 kDa cut-off concentrators (Corning, New York, USA) and then run over a 120 mL Superdex 75 pg HiLoad 16/600 column equilibrated with 20 mM NaPi, 150 mM NaCl, pH 7.0. Purified holo protein was frozen with liquid N₂ and stored at −80 °C until further use.

2.2.2. Expression and purification of HasAp

Plasmid encoding Haem acquisition system A from *Pseudomonas aeruginosa* (HasAp) was acquired from Invitrogen (Massachusetts, USA). The plasmid was transformed into *Escherichia coli* BL21 pLysS strain,

which was grown aerobically in 0.5 L LB medium containing 0.1 mM kanamycin and 0.1 mM chloramphenicol in a 2 L flask at 37 °C, 250 rpm. Protein expression was induced at an OD_{600} of 0.8–1.0 using 1 mM IPTG and growth was continued overnight at 30 °C. The protein was harvested as in section 2.2.1. Cell debris was removed via ultracentrifugation (Beckman Coulter Optima XE-90) at 30k rpm, 30 min, 4 °C. Purification was performed over a Q column as in section 2.2.1 and collected fractions were selected using SDS-PAGE. The pooled fractions were concentrated in a 3 kDa cut-off concentrator (Macrosep Advance Centrifugal Device Pall Corporation, New York, USA). Dialysis was performed against 4 L of 50 mM NaPi and 0.7 M NH$_4$SO$_4$, pH 7.0 at 4 °C overnight as in section 2.2. This was followed by purification over a butyl column (5 mL HiTrap Butyl FF Sigma Aldrich, Missouri, USA) equilibrated with 50 mM NaPi and 0.7 M (NH$_4$)$_2$SO$_4$, pH 7.0. Holo HasAp is eluted with 50 mM NaPi and 0.5 M (NH$_4$)$_2$SO$_4$, pH 7.0 and apo HasAp was eluted with a gradient to 20 mM NaPi, pH 7.0 over 100 mL. Fractions of holo protein and fractions of apo protein were combined separately, concentrated, purified over a size exclusion column, then stored as in section 2.2.1.

2.3. Preparation of apo protein and binding of the complexes

2.3.1. Haem extraction from Mb and CB5 via Teale's method

Haem extraction from cytochrome B5 and myoglobin was performed using Teale's method [27]. In short, the pH of the protein was lowered to pH 2.0, by dropwise addition of 0.5 M HCl under constant stirring on ice. An equal volume of cold 2-butanone was added and mixed, then pipetted off after the layers separated, and this procedure was repeated a second time. The aqueous layer was pipetted directly into a 3.5 kDa cut-off dialysis bag (cellulose dialysis tubing from Spectrum Chemical, California, USA) and dialyzed against 2 L of 20 mM NaPi, pH 6.5, 7.0, 7.5 or 8.0 at 4 °C overnight. The dialysis buffer was exchanged once after 2 h of dialysis. UV–Vis was used to verify the protein was in the apo-state.

2.3.2. Haem extraction from HasAp via the cold acid acetone method

Haem extraction from HasAp was accomplished via the cold acetone acid method [28,29]. In short, 1 mL of holo HasAp was added dropwise to 50 mL of cold solution of 0.2% HCl in acetone that was kept at −20 °C, under constant stirring on ice. The protein was pelleted in an Eppendorf centrifuge (10000×*g*, 30 min, −9 °C, Eppendorf centrifuge 5804 R) and then resuspended in 7 M urea, 0.1 M Tris-HCl, pH 7.5 to a final concentration of 2–5 μM apo HasAp. This was pipetted into a 3.5 kDa cut-off dialysis bag and dialyzed against 2 L of 0.1 M Tris-HCl pH 7.5, 0.1 M NaCl at 4 °C overnight. Apo protein was frozen with liquid N$_2$ and stored at −80 °C until further use. UV–Vis was used to verify the protein was in the apo-state. The buffer was exchanged to 20 mM NaPi, pH 6.5, 7.0, 7.5 or 8.0 via re-concentration using 0.5 mL Amicon spin concentrators with 3 kDa MWCO from Merck Millipore (Massachusetts, USA) before use.

2.3.3. Incubation with metal complexes

The apo proteins were reacted with the transition-metal catalysts by mixing 10 μM of the apo protein in 20 mM NaPi buffer at pH 6.5, 7.0, 7.5 or 8.0 with 10 μM, 50 μM or 100 μM catalyst (protein: catalyst molar ratio 1:1, 1:5 or 1:10) by adding 5 μL of catalyst to 45 μL of protein solution. All reactions were performed over 24–48 h at 4 °C under constant agitation in the dark. In all experiments in which only complexes Co1 and/or Co2 were used, they were dissolved in dimethyl formamide (DMF). A final concentration of 10% DMF was present in all samples used in these experiments. In experiments including the full library of Ru- and Co-complexes; complexes Co1, Co3 and Ru1 were dissolved in distilled water Co4, Ru2, and Ru3 in dimethyl sulfoxide (DMSO) and Co2 in 60% DMSO, 40% distilled water.

2.4. Gel electrophoresis

(Semi-)(Native) Gel electrophoresis was performed using 15% polyacrylamide gels. Denaturing and semi-native gels contained 0.1% sodium dodecyl sulphate (SDS) in both gel and running buffer. Cracking buffer for native and semi-native PAGE was prepared in absence of SDS and β-mercaptoethanol. Denaturing and semi-native gels were run (Mini-Protean System and PowerPac Basic Power Supply from Bio-Rad, California, USA) for 50 min at 200 V. Gels loaded with HasAp were run at 100 V, 90 min as longer exposure to SDS was required due to the high stability of the protein. All native gels were run for 90 min at 100 V. The gels were imaged with 2,2,2-Trichloroethanol (5 μL per mL was added to the gel mixture, sigma Aldrich) [30], using a Gel Doc XR+ from Bio-Rad and processed using the ImageLab software (version 6.0.1, Bio-Rad). Gel images (Figs. 2, 3 and 5) were processed using the Image lab Software version 6.01 from Bio-Rad, adjusting the gamma setting to improve the contrast.

2.5. ESI-MS

ESI-MS was performed on a Synapt G2-Si mass spectrometer from Waters (Massachusetts, USA), initial separation and denaturing of protein samples is achieved using a C4 polymeric reversed phase UPLC column. Samples were buffer-exchanged to 10 mM NH$_4$Ac buffer, pH 7.0 a using Micro Bio-Spin p6 gel desalting columns from Bio-Rad (California, USA), maximally 30 min before loading. Deconvolution of spectra was performed using the MaxEnt. Algorithm [31] of the MassLynx MS Software.

3. Results

Three haem-binding proteins were selected, cytochrome B5 (CB5), myoglobin (Mb) and Haem acquisition system A from *Pseudomonas aeruginosa* (HasAp) (Fig. 1), that were reacted with cobalt based transition metal complexes (Fig. 2). To this end each protein was prepared in the apo (haem-free) state using Teale's method for CB5 and Mb and the cold acid acetone method for HasAp to be able to bind a synthetic cobalt complex in its haem binding pocket.

3.1. Comparison of denaturing, semi-native and native PAGE for detecting protein catalyst interaction

We compared the ability of semi-native PAGE to analyse the binding of different cobalt complexes to proteins with conventional (denaturing) SDS-PAGE and with native PAGE. Hereto we performed SDS, semi-native and native PAGE gel runs of CB5, Mb, and HasAp that were each mixed with the complexes Co1 and Co2 (Fig. 2). The first lanes on the gels in Fig. 2 contain the holo- (haem bound) and apo form of each protein (lane H and A, respectively), followed by the apo proteins mixed with increased amounts of catalysts Co1, in lane 2–4, or Co2, in lane 5–7.

In the denaturing gels in Fig. 2, panel 1, no changes can be observed with either complex. The apo-, holo- and complex-modified proteins all run at the same height corresponding to the apo protein molecular weight, with the exception of holo HasAp for which two bands are observed, due to its increased resistance to denaturation that will be discussed in section 4.2. The results indicate that conventional SDS-PAGE gel analyses, where proteins are denatured and band separation is solely based on differences in molecular weight, is not suitable for detection of binding of small metal complexes.

In contrast, the native PAGE gel run (Fig. 2, panel 3) shows differences between the heights of the apo- and holo-protein bands and shows band changes for each of the apo proteins mixed with Co1 at 1:5 and 1:10 protein to complex ratios, and for apo Mb mixed with Co2 at 1:5 and 1:10 ratios. The bands of the holo proteins are shifted down on native gel relative to the migration of the apo protein bands. At increasing concentrations of Co1, the apo protein bands of CB5 and of
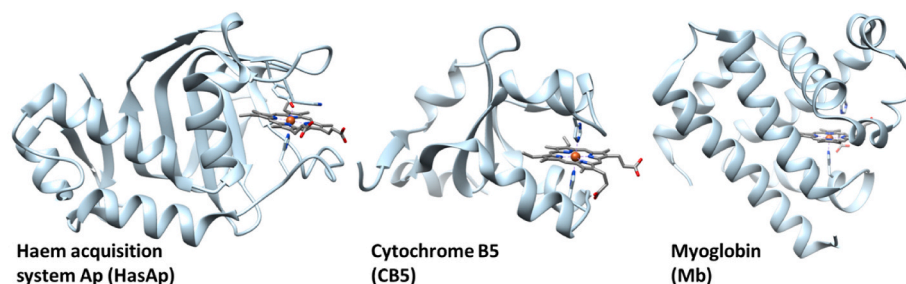
Fig. 1. Haem proteins used in this study, from left to right: Haem acquisition system A from *Pseudomonas aeruginosa* (HasAp, PDB 3ELL), bovine cytochrome B5 (CB5, PDB 1CYO) and equine skeletal Myoglobin (Mb, PDB 5D5R).
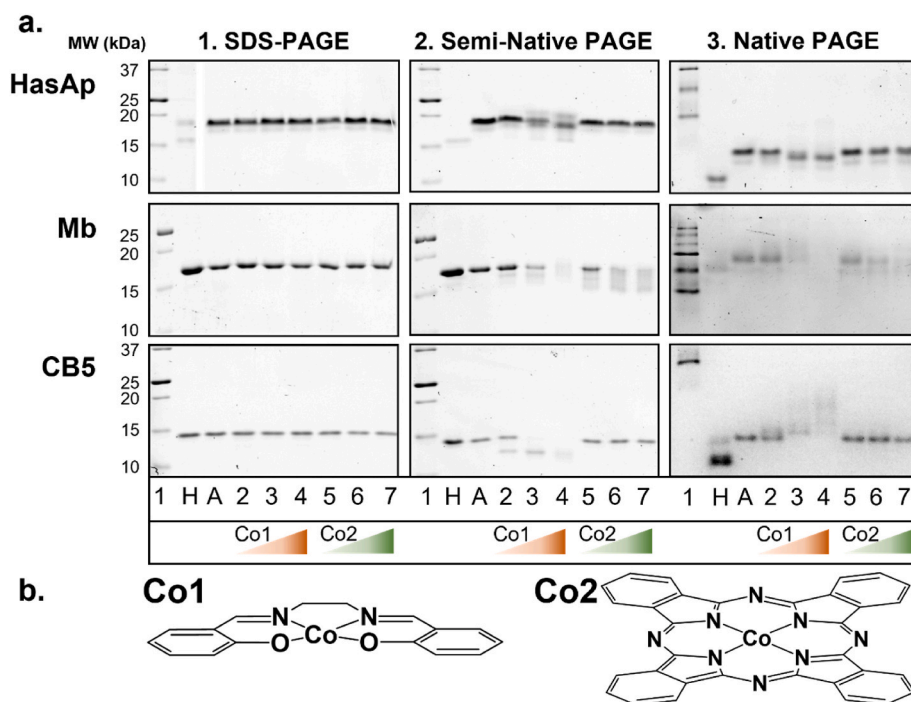

Fig. 2. a. Denaturing (panel 1.), semi-native (panel 2.) and native (panel 3.) PAGE of HasAp (top), Mb (middle) and CB5 (bottom). Samples were prepared by mixing 10 μM apo protein in 20 mM NaPi, pH 8.0 with [N,N′-bis(salicylidene)ethane-1,2-diaminato]cobalt(II) (Co1) or cobalt(II) phthalocyanine (Co2) catalyst at 4 °C for 24 h. On each gel lane 1 is the protein ladder with molecular weight indicated on the left, H is the holo form, A is the apo form, 2–4 are protein with added Co1 10 μM, 50 μM and 100 μM (protein: catalyst molar ratio 1:1, 1:5 and 1:10, indicated with the orange gradient), 5–7 are protein with added Co2 10 μM, 50 μM and 100 μM (ratio 1:1, 1:5 and 1:10, indicated with the green gradient). b. Chemical structures of Co1 and Co2. (For interpretation of the references to colour in this figure legend, the reader is referred to the Web version of this article.)

Mb are progressively replaced by slower migrating protein bands that appear as a smear, and in case of the 1:10 ratio Mb:Co1 the band signals disappear completely. The SDS-PAGE gel image (panel 1, Mb and CB5, lanes 3 and 4) of the same samples however reveals that the proteins are not degraded, as a sharp band is observed for each case, with the heights corresponding with the apo protein weights. It is therefore hypothesized that the observed smearing or fading is caused by protein oligomerization, or by binding of Co1 to multiple protein sites, giving a distribution of proteins with different gel-migration properties. For all HasAp samples two bands are observed, one strong band and a lighter band just below. The origin of those two bands will be discussed in section 3.3. Mixtures of HasAp with Co1 at 1:5 or 1:10 ratios show two bands that migrate faster than those of the apo protein.

The semi-native gel (Fig. 2, panel 2) shows band changes for each of the apo proteins mixed with Co1 and for apo Mb mixed with Co2. For all the three proteins, one or more new bands below the height of the apo protein band emerge at increasing Co1 concentrations, while for HasAp, also a band above the height of the apo protein band is observed. Similar to the results of the native gel run, band signals fade out for samples of Mb and CB5 mixed with Co1 at increased Co1 concentrations.

3.2. Effect of pH

To investigate the effect of pH, each apo protein was mixed in a 1:1

(mol/mol) ratio with complex Co1 in buffers at pH 6.5, 7.0, 7.5 and 8.0. Fig. 3 shows the denaturing, semi-native and native PAGE gel images of the mixtures prepared under varying pH conditions. In the semi-native PAGE gel image, for Mb a clear pH trend can be observed where the relative intensity of the second protein band that runs below the apo protein band, increases at lower pH. Neither the denaturating nor the native gel images of Mb show a significant effect of pH.

Based on the results of SDS-, semi-native and native PAGE gel analysis, we formulate the working hypothesis that the metallo-protein complexes migrate differently on semi-native gel than the apo protein, so that they can be distinguished on gel. To test and validate our working hypothesis formulated on the basis of the gel analyses, we made a comparison with electron spray ionization mass spectrometry (ESI-MS) as described in the next paragraph.

3.3. Electron spray ionization mass spectrometry (ESI-MS)

Fig. 4 presents the deconvoluted ESI-MS spectra of HasAp, Mb and CB5 reacted with Co1 and Co2 in a 1:5 molar ratio. The mass spectra show that Co1 binds to all the three proteins, while Co2 only binds to Mb. According to the ESI-MS data, Co1 binds to HasAp and Mb in 1:1 stoichiometry, while for CB5 also a significant signal of 1:2 (protein: complex) stoichiometry is observed. Two peaks are observed for CB5 binding to Co1 in 1:2 stoichiometry (Fig. 4c); one corresponding with
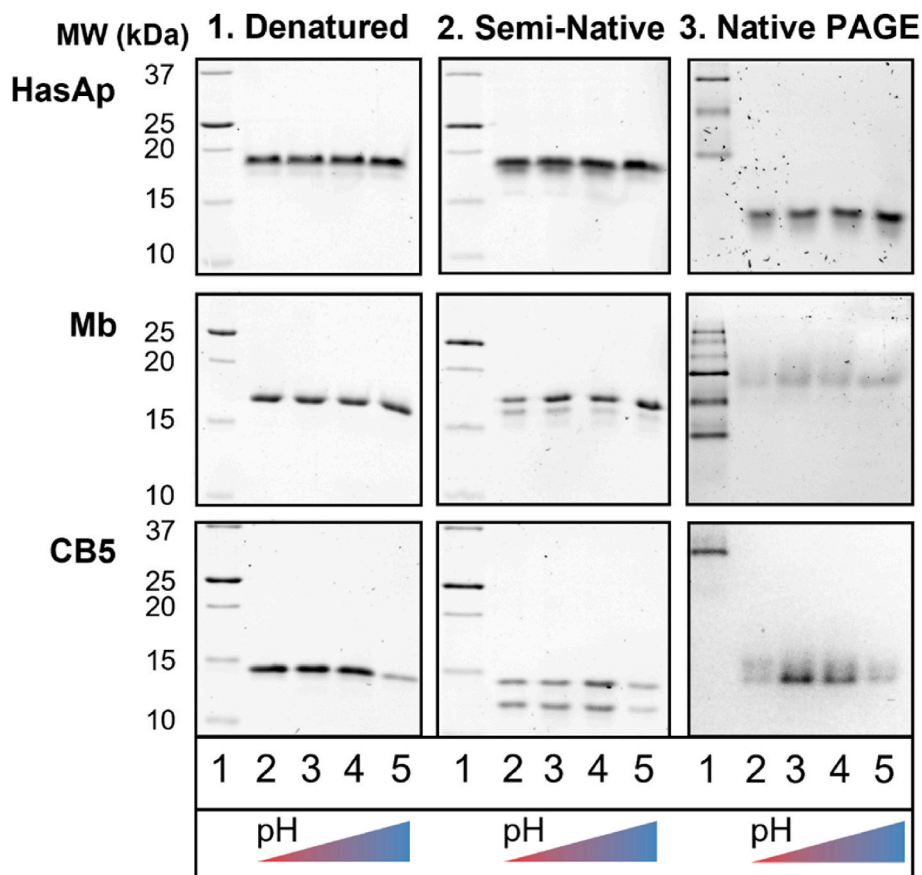
Fig. 3. Denaturing (panel 1.), semi-native (panel 2.) and native (panel 3.) PAGE of HasAp (top), Mb (middle) and CB5 (bottom). Samples were prepared by mixing 10 μM apo protein in 20 mM NaPi, pH 6.5, 7.0, 7.5 or 8.0 with 10 μM Co1 (protein: catalyst ratio 1:1)) at 4 °C for 24 h. On each gel lane 1 is the protein ladder with molecular weight indicated on the left, lanes 2–5 are the protein catalyst mixture at pH 6.5, 7.0, 7.5 and 8.0 respectively.

the molar mass of the apo protein plus two Co1, and one with additional molar mass of 28 Da. The extra mass could represent the (axial) coordination of CO to one of the bound Co1 complexes, as CO is a possible breakdown product of dimethylformamide (DMF) [32–34], which was used as a solvent in this experiment. According to mass spectroscopy, only Mb was shown to bind Co2. The mass spectrum of Mb mixed with Co2 shows two peaks, one corresponding with the mass of the apo protein and the other corresponding with the mass of the apo protein and Co2 plus an additional mass of 26 Da. The latter peak corresponds with the mass of the apo protein plus Co2 plus CO minus two protons, and could represent Mb binding to Co2 with axial coordination of CO.

ESI-MS was further performed on apo CB5 reacted with Co1 in 1:1 and 1:10 ratios, of which the resulting spectra are shown in Fig. S1 in the SI section. The spectrum of CB5–Co1 reacted using a 1:1 protein to complex mixture shows a population of apo CB5 and of CB5 binding one Co1 complex, and a very small fraction of CB5 binding two Co1 (CB5–2Co1). For the 1:10 protein to complex reaction mixtures, significant over-binding is observed where CB5 binds 2 or 3 Co1 (CB5–2Co1, CB5–3Co1). The CB5–2Co1 and CB5–3Co1 peaks each contain an additional mass of 28 Da attributed to CO. No additional 28 Da mass is observed for CB5 binding only one Co1, implying that no axial binding site is available for CO binding when Co1 binds to CB5 in a 1:1 stoichiometry, conform with binding of Co1 into the haem binding pocket.

Mb is the only protein tested that binds to Co2. In the native holo conformation of Mb the haem is coordinated from one side by histidine and the other by water H-bonded to a neighbouring histidine [35,36]. While coordinated water is not observed in the mass spectrum for Mb-Co2 nor for Mb-Co1, an extra mass of 26 Da attributed to CO (minus two protons) was observed for Mb-Co2. This, however, does not prove that binding of Co2 has taken place outside of the binding pocket, since

coordination by Mb in the binding pocket could be one-sided [37].

Summarizing, the ESI-MS results are consistent with the patterns observed on semi-native gel. Band changes on semi-native gel are observed for all three proteins mixed with Co1 and only for Mb mixed with Co2, supporting our working hypothesis that binding of metal complexes influences the migration of proteins through semi-native gel, separating them from the apo proteins.

To gain more insight into the properties of the complex bound protein, we analysed the chromatograms of protein runs over a C4 column that are performed prior to the ionization in the ESI-MS experiment. The C4 column is a hydrophobic interaction column from which proteins will be eluted with retention times increasing with hydrophobicity. For CB5 and Mb reacting with Co1 and Co2 only small changes in retention times are observed compared to those of the apo protein (Figures S2 and S3, SI section), and the retention times of the holo and apo protein are similar. However, for Mb-Co2 a distinct new peak is observed compared to apo Mb that can be deconvoluted (Fig. S3a and c., SI section). Deconvolution of the first peak reveals only apo Mb (data not shown) and deconvolution of the second peak reveals bound Mb-Co2 (Fig. 4e.). The longer retention time indicates that the Mb-Co2 protein complex is more hydrophobic than apo Mb. Co2 is hydrophobic and the increased hydrophobicity of the complex-bound protein suggests that the catalyst is bound to the protein surface, outside the haem binding pocket.

The chromatograms of HasAp are more complex to interpret (Figs. S4 and SI section). Two peaks are observed in the C4 chromatogram of the apo protein, one at 10.62 min, with a large tail resulting from the "stickiness" of the protein to the hydrophobic column, and a second much smaller peak at 22.93 min. A similar pattern is observed in all three gel-types in Fig. 2, where a faint second, lower band can be observed in apo HasAp. Deconvolution of each peak, including the tail of
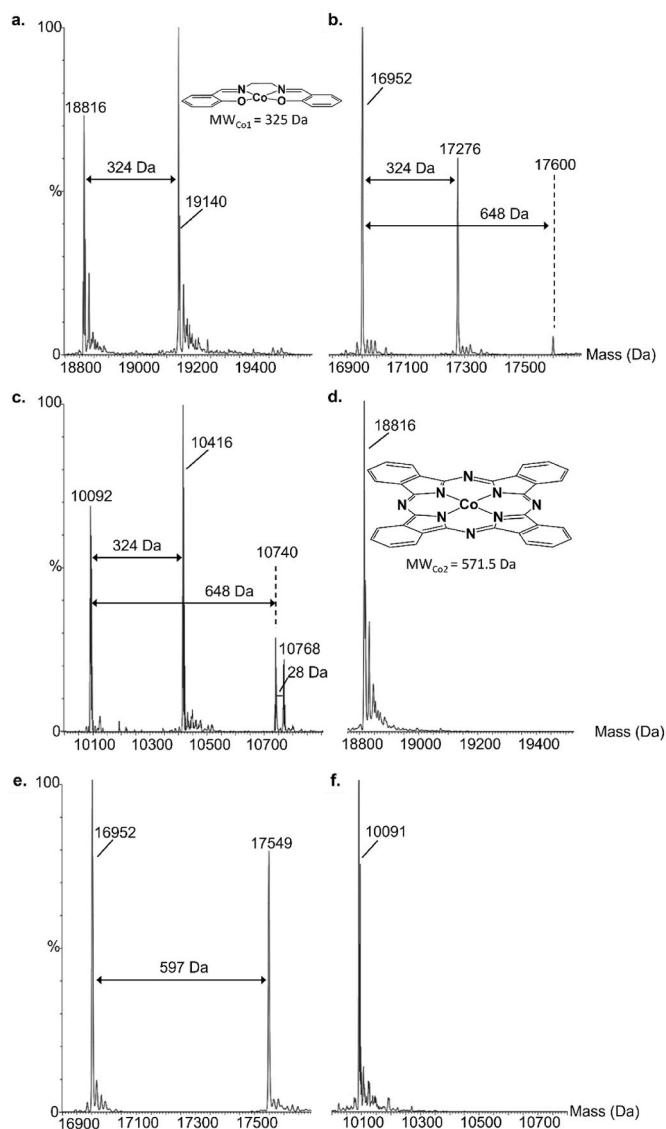
Fig. 4. ESI mass spectrometry of HasAp, Mb, and CB5 with Co1 (a, b, and c respectively) and Co2 (d, e, and f respectively). Samples were prepared by mixing 10 μM apo protein in 20 mM NaPi, pH 8.0 with 50 μM (protein: catalyst ratio 1:5) of Co1 (top) or Co2 (bottom) catalyst at 4 °C for 24 h. The molar mass in Da of each peak and the differences in molecular mass between the observed peaks are given in the figure. The molecular structure of catalyst Co1 is shown in panel a., with its molecular mass, the structure and mass of Co2 are shown in panel d.

the 10.62 min peak, reveals that both peaks contain protein with the molar mass of apo HasAp. We assume that the small hydrophobic fraction of apo HasAp that elutes at ~23 min is either (partially) unfolded protein or reflects a more open conformational state of the apo protein. For holo HasAp, instead, a 6.80 min peak is observed, relating to more hydrophilic protein, that we assume to be the closed, haem-containing, conformation of HasAp. An ~11 min peak is also observed in the run of holo HasAp, which is assigned to the open, haem-free, conformation, indicating that some of the haem was removed. For HasAp reacted with Co1, three retention times are observed; the ones at ~11 min and ~23 min, that are similar to those observed in apo HasAp, and one at 6.55 min that is similar to the retention time of holo HasAp. Although no binding of Co2 to HasAp is observed in the deconvoluted ESI-MS and gel results, the C4 chromatogram of HasAp reacted with Co2 surprisingly shows two extra retention peaks at 6.70 and 7.25 min in addition to the retention peaks that can be attributed to the apo protein. Deconvolution

of these two peaks reveals only apo HasAp (data not shown). Conformational heterogeneity of Co2-HasAp as expressed by its two retention peaks in the C4 chromatogram may explain why this complex is not detected on gel, as the presence of multiple conformations could result in a faint smear rather than a clear band.

3.4. Comparing first- and second-row transition metal complex binding

In sections 3.1 and 3.2 it was demonstrated that semi-native PAGE analysis is applicable for evaluating the binding of two types of Co-containing metal complexes to three types of proteins. To further investigate the applicability of the semi-native gel screening method, we reacted apo CB5 with two other Co-containing complexes and with 3 types of Ru-containing catalyst complexes and analysed those by semi-native PAGE (Fig. 5). For comparison, samples of CB5 reacted with Co1 and with Co2 were also loaded on the same gel. The appearance of new bands is observed for apo CB5 reacted with the Ru-containing complexes Ru2 and Ru3 and for reactions of apo CB5 with Co-containing complexes Co1, Co3 and Co4, suggesting that Ru2, Ru3, Co1, Co3 and Co4 can bind to CB5, while Ru1 and Co2 cannot. Mass spectrometry was performed on the mixtures for which new bands could be observed on gel. The ESI-MS results are shown in Fig. S5 panels a through d, SI section and confirm binding of Co3, Co4 and Ru2 to apo CB5 in 1:1 stoichiometries and in the case of Ru2 also in 1:2 and 1:3 stoichiometries.

For the reaction of apo CB5 with Ru2, mass peaks are observed with the following increases in mass with respect to the mass of apo CB5: 448 Da, 890 Da and 1339 Da. The additional mass of 448 Da may be assigned to binding of the Ru2 compound minus its axial water ligand plus 3 additional protons; the additional mass of 890 Da corresponds to the mass of 2 Ru2 compounds minus 2 axial waters and minus 1 proton; the mass increase of 1339 Da corresponds with 3 Ru2 compounds minus 3 water molecules plus 3 additional protons.

For samples of apo CB5 reacted with Co3 or Co4 in a 1:10 ratio, a second peak is observed in addition to a peak corresponding to the mass of apo CB5, with an additional mass of 368 Da. We assign the additional mass to Co3 or Co4 minus its axial ligands minus 1 proton, indicating that apo CB5 is capable of binding to Co3 and Co4 in a 1:1 ratio. We can thus conclude that Co3 and Co4 each lose their axial ligands upon binding and are therefore likely being coordinated in the binding pocket, whereas Ru2 binds in higher ratios and loses a water axial ligand while a CO remains bound.

The mass spectrum of apo CB5 reacted with Ru3 shows a peak of the apo protein together with higher molecular weight fractions that do not match with the additional mass of the Ru3 catalyst (Figs. S5b and SI section). We considered that the protein may be cut by this specific catalyst, as some of the more intense peaks match with the full Ru3 complex containing both axial ligands plus apo CB5 minus 1–3 amino acids at the C terminus (Arg and 1 or 2 Asp). In the mass spectrum, peaks at 10420 Da, 10305 Da and 10190 Da match with the weights of CB5–Ru3 minus Arg, CB5–Ru3 minus Arg-Asp, CB5–Ru3 minus Arg-Asp-Asp respectively.

The C4 chromatograms of CB5–Co3 and CB5–Co4 1:10 (Fig. S6 d and e, SI section) look identical, containing a single peak with retention time 11.61 min. In the chromatogram of apo CB5 reacted with Ru2 (Fig. S6 b, SI section) new peaks are observed with longer retention times than that of the apo protein, indicating that binding of Ru2 to CB5 has a clear effect on its hydrophobicity. Individual deconvolution of each peak (not shown) reveals that the fractions contain CB5 with 0, 1, 2 or 3 Ru2 complexes bound respectively. This clear increase of hydrophobicity upon binding each Ru2 is consistent with its binding to the exterior of the protein (i.e. to the outer histidines of CB5: His20, His31 and His85). The appearance of smeared bands on semi-native gel for apo CB5 + Ru2 may also be explained by the multiple binding stoichiometries. The chromatogram of apo CB5 reacted with Ru3 in a 1:10 molar ratio (Fig. S6 c, SI section) contains only one peak with a retention time 11.66
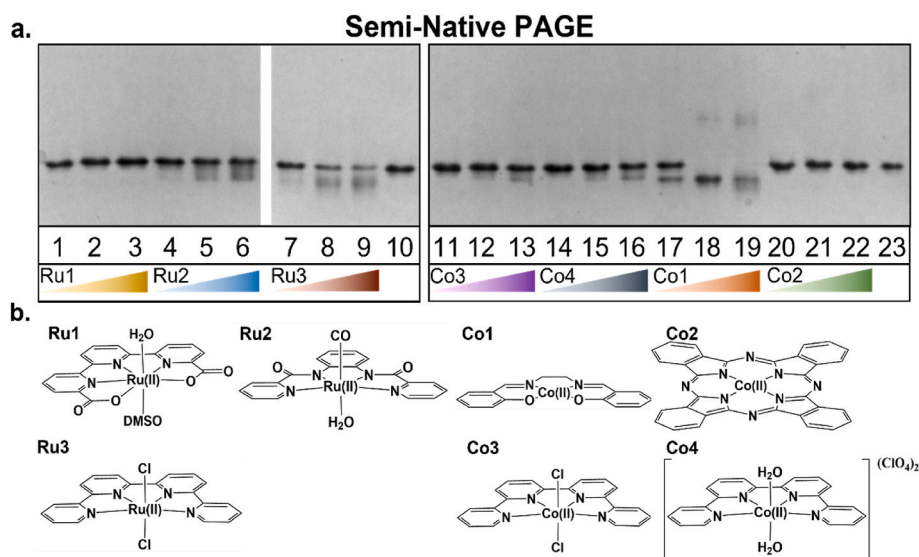
Fig. 5. a. Semi-native PAGE of apo CB5 reacted with different catalysts. Samples were prepared by mixing 10 μM apo CB5 in 20 mM NaPi, pH 7.4 with 10 μM, 50 μM or 100 μM of catalyst (protein: catalyst ratio 1:1, 1:5 and 1:10) at 4 °C for 48 h. Lane 1–3 are apo CB5 + Ru1, 4–6 are apo CB5 + Ru2, 7–9 are apo CB5 + Ru3, Lane 10 is apo CB5, 11–13 are apo CB5 + Co3, 14–16 are apo CB5 + Co4, 17–19 are apo CB5 + Co1, 20–22 are apo CB5 + Co2 and 23 is apo CB5. b. Chemical structures of Ru1 through Ru3 and Co1 through Co4.

min, which is a somewhat shorter than that of apo CB5, indicating that the reaction product is slightly more hydrophilic.

4. Discussion

A combined gel and ESI-MS analysis was performed on three different proteins that were reacted with first- and, for apoCB5, also second-row transition metal complexes. The results consistently show that protein-metal complex interactions, confirmed by ESI-MS, are visible as band changes on semi-native PAGE gels where the complexed proteins migrate faster or slower than the apo proteins. The denaturing PAGE results confirm that under all conditions, the proteins remained intact so that the band changes cannot be attributed to degradation. In a semi-native PAGE experiment, the protein sample is prepared in absence of SDS, as for a native sample, and is exposed to the denaturing properties of SDS present in the gel upon gel loading. The protein therefore will denature as it migrates through the gel. The rate of denaturation is influenced by the stability and compactness of the proteins, which are affected by metal complex binding, especially when the complexes are stabilized inside the haem pockets, leading to protein conformational changes. The position on semi-native gel as such is a measure of the resistance against protein denaturation. The observation of new lower bands with respect to the original apo protein band can be explained by stabilizing protein-complex interactions whereas the observation of new, higher bands could indicate destabilizing interactions or the formation of sufficiently SDS-resistant oligomers. In native PAGE experiments, no denaturing agents are used, and the rate of gel migration may be influenced by multiple factors, i.e. protein oligomerization, conformational changes and changes in charge distributions. Indeed, CB5 reacted with Co1 in a 1:1 ratio clearly detects a second band of complex-bound protein on semi-native gel, while the native gel only shows band changes at higher Co1 concentrations, at which, according to the ESI-MS data results, over-binding occurs.

Mb, HasAp, and CB5 each have a different relationship between coordination of the native haem ligand and structural stability. Cytochrome B5 coordinates haem with two axial histidines and partially unfolds when haem is lost [38]. Mb coordinates haem with one histidine and one water molecule that is H-bonded to a distal histidine and the protein structure is preserved when haem is removed [39,40]. Finally, HasAp is a transient haem binding protein that coordinates haem with one histidine and one tyrosine and has an opening and closing mechanism to capture haem by switching its fold between an open and closed conformation [41]. Mb has a more stable native holo-fold than CB5 [36,

42,43] and both the closed and open forms of HasAp are more stable than the other two proteins [44]. These differences in stability and the dependence of the protein fold on the presence of a coordinated ligand could explain the observed differences on semi-native gel. For HasAp, which retains a stable fold in its apo-state, the difference in gel band heights of the complex-bound and apo-protein is small, while for CB5, which unfolds in the apo-state, the difference is large, suggesting a larger increase in stability of apo CB5 upon complex binding.

CB5 was further screened against a library of transition metal catalysts to show the general applicability of the semi-native gel method for analysing protein-metal complex interactions. This screening revealed the importance of the choice of axial ligands of the metal complexes prior to binding the protein (Fig. 5). A trend is observed where catalysts with Cl and H_2O ligands bind well, while catalysts with DMSO or CO ligands do not. Catalysts Co3 and Co4 that have Cl and H_2O ligands, respectively, are capable of binding into the haem binding pocket of CB5, according to their loss of both axial ligands upon binding. Ru2, which has one H_2O and one CO ligand, binds to the protein with one sided coordination. The CO ligand remained bound to the protein-catalyst complex (1 CO per Ru2 catalyst), which can be ascribed to the strong π-back bonding interaction between the CO-ligand and metal centre. Ru3 has two Cl ligands, but appeared to cleave the protein as discussed in section 3.4. Ru1 has one H_2O and one DMSO axial ligand, yet Ru1 did not bind to apo CB5. The reason may be steric in nature as Ru1, which has at least one good leaving ligand (H_2O), is slightly bulkier than Ru2, which is able to bind with only one good leaving ligand. Co1 and Co2 both lack axial ligands, here instead the influence of the planar ligands is observed. The size of Co2 may have been too large to enter the binding pockets of HasAp and CB5, while the much smaller Co1 binds very well to all three proteins.

5. Conclusion

We successfully developed a rapid screening method based on semi-native gel electrophoresis, that is generally applicable for study of the interaction between small molecule metal complexes and proteins. Contrary to SDS and native PAGE, semi native PAGE could reliably detect the binding of small metal complexes to proteins. Semi-native gel analysis requires small sample amounts (only 0.5 μg of protein), does not rely on UV–Vis spectral changes of the metal complexes upon protein interaction and does not require specialized equipment. With our screening method, we assessed the interaction of several Co- and Ru-based water-oxidation catalysts with three types of haem proteins. The

analysis was completed by ESI-MS to determine the present binding stoichiometries and complex axial coordination inside a protein pocket.

Declaration of interests

Declarations of interest: none.

Funding

CRediT author statement

Conceptualization and methodology were done by LO, EPR, AP and SB. LO, EPR, CB, NL and BR carried out the experiments. LO, AP, EPR, SB wrote the original draft. AP and SB supervised the project. All authors have read and approved the final manuscript.

Acknowledgements

Appendix A. Supplementary data

Deconvoluted mass spectra of CB5 reacted with Co1 in ratio's 1:1, 1:5 and 1:10 are shown in Fig. S1, the C4 chromatograms of protein in the holo and apo-states and in after reacting with a 1:5 molar ratio of Co1 or Co2 are given for CB5, Mb and HasAp respectively in Figures S2 through S4, the deconvoluted mass spectra of CB5 reacted with catalysts Ru2, Ru3, Co3 and Co4 are given in Fig. S5 and the related C4 chromatograms are provided in Fig. S6.

Appendix B. Supplementary data

Supplementary data to this article can be found online at https://doi.org/10.1016/j.ab.2022.114788.

References

[1] T. Ueno, S. Abe, N. Yokoi, Y. Watanabe, Coordination design of artificial metalloproteins utilizing protein vacant space, Coord. Chem. Rev. 251 (21–24) (2007) 2717–2731.

[2] F. Schwizer, et al., Artificial metalloenzymes: reaction scope and optimization strategies, Chem. Rev. 118 (1) (Jan. 2018) 142–231, https://doi.org/10.1021/acs.chemrev.7b00014.

[3] T. Ueno, et al., Design of artificial metalloenzymes using non-covalent insertion of a metal complex into a protein scaffold, J. Organomet. Chem. 692 (1–3) (2007) 142–147.

[4] M. Ohashi, T. Koshiyama, T. Ueno, M. Yanase, H. Fujii, Y. Watanabe, Preparation of artificial metalloenzymes by insertion of chromium (III) Schiff base complexes into apomyoglobin mutants, Angew. Chemie Int. Ed. 42 (9) (2003) 1005–1008.

[5] C. Shirataki, et al., Inhibition of heme uptake in Pseudomonas aeruginosa by its hemophore (HasAp) bound to synthetic metal complexes, Angew. Chem. 126 (11) (2014) 2906–2910.

[6] Y. Shisaka, et al., Hijacking the heme acquisition system of Pseudomonas aeruginosa for the delivery of phthalocyanine as an antimicrobial, ACS Chem. Biol. 14 (7) (2019) 1637–1642.

[7] H. Wójtowicz, M. Bielecki, J. Wojaczyński, M. Olczak, J.W. Smalley, T. Olczak, The Porphyromonas gingivalis HmuY haemophore binds gallium (III), zinc (II), cobalt (III), manganese (III), nickel (II), and copper (II) protoporphyrin IX but in a manner different to iron (III) protoporphyrin IX, Metallomics 5 (4) (2013) 343–351.

[8] K.K. Chandel, S. Pahadiya, Sodium Dodecyl Sulfate-Poly Acrylamide Gel Electrophoresis, 2005.

[9] A. Chrambach, D. Rodbard, Polyacrylamide gel electrophoresis, Science (80-.) 172 (3982) (1971) 440–451.

[10] J.L. Brunelle, R. Green, Chapter twelve - one-dimensional SDS-polyacrylamide gel electrophoresis (1D SDS-PAGE), in: J. Lorsch (Ed.), Laboratory Methods in Enzymology: Protein Part C, vol. 541, Academic Press, 2014, pp. 151–159.

[11] C. Arndt, S. Koristka, H. Bartsch, M. Bachmann, Native polyacrylamide gels, in: Protein Electrophoresis, Springer, 2012, pp. 49–53.

[12] R. Voulhoux, M.P. Bos, J. Geurtsen, M. Mols, J. Tommassen, Role of a highly conserved bacterial protein in outer membrane protein assembly, Science (80-.) 299 (5604) (2003) 262–265.

[13] J. Jiang, J.K. Davies, T. Lithgow, R.A. Strugnell, K. Gabriel, Targeting of Neisserial PorB to the mitochondrial outer membrane: an insight on the evolution of β-barrel protein assembly machines, Mol. Microbiol. 82 (4) (2011) 976–987.

[14] B. Lugtenberg, J. Meijers, R. Peters, P. van der Hoek, L. van Alphen, Electrophoretic resolution of the 'major outer membrane protein' of Escherichia coli K12 into four bands, FEBS Lett. 58 (1–2) (1975) 254–258.

[15] L.Z. Robinson, N. Reixach, Quantification of quaternary structure stability in aggregation-prone proteins under physiological conditions: the transthyretin case, Biochemistry 53 (41) (2014) 6496–6510.

[16] Y. Wakita, et al., Characterization of non-amyloidogenic G101S transthyretin, Biol. Pharm. Bull. 41 (4) (2018) 628–636.

[17] H.J. Bigus, P. Voss, J. Krause-Bonte, H. Stransky, G. Gauglitz, A. Hager, Light-dependent assembly of pigment-protein complexes in etiolated leaves of Phaseolus coccineus L. monitored by seminative gel electrophoresis, fluorescence spectroscopy and pigment analysis, J. Plant Physiol. 147 (3–4) (1995) 408–418.

[18] E.S. Athlan, W.E. Mushynski, Heterodimeric associations between neuronal intermediate filament proteins, J. Biol. Chem. 272 (49) (1997) 31073–31078.

[19] J.N. Henderson, J. Zhang, B.W. Evans, K. Redding, Disassembly and degradation of photosystem I in an in vitro system are multievent, metal-dependent processes, J. Biol. Chem. 278 (41) (2003) 39978–39986.

[20] T. Hoang, M.D. Smith, M. Jelokhani-Niaraki, Expression, folding, and proton transport activity of human uncoupling protein-1 (UCP1) in lipid membranes: evidence for associated functional forms, J. Biol. Chem. 288 (51) (2013) 36244–36258.

[21] C. Galaup, J.-M. Couchet, S. Bedel, P. Tisnès, C. Picard, Direct access to terpyridine-containing polyazamacrocycles as photosensitizing ligands for Eu (III) luminescence in aqueous media, J. Org. Chem. 70 (6) (2005) 2274–2284.

[22] R. Matheu, J. Benet-Buchholz, X. Sala, A. Llobet, Synthesis, structure, and redox properties of a trans-diaqua Ru complex that reaches seven-coordination at high oxidation states, Inorg. Chem. 57 (4) (Feb. 2018) 1757–1765, https://doi.org/10.1021/acs.inorgchem.7b02375.

[23] M.D. Kärkäs, T. Åkermark, H. Chen, J. Sun, B. Åkermark, A tailor-made molecular ruthenium catalyst for the oxidation of water and its deactivation through poisoning by carbon monoxide, Angew. Chemie Int. Ed. 52 (15) (2013) 4189–4193.

[24] E. Wachter, A. Zamora, D.K. Heidary, J. Ruiz, E.C. Glazer, Geometry matters: inverse cytotoxic relationship for cis/trans-Ru(ii) polypyridyl complexes from cis/trans-[PtCl2(NH3)2], Chem. Commun. 52 (66) (2016) 10121–10124, https://doi.org/10.1039/C6CC04813G.

[25] Y. Liu, et al., Catalytic water oxidation by ruthenium (II) quaterpyridine (qpy) complexes: evidence for ruthenium (III) qpy-N, N‴-dioxide as the real catalysts, Angew. Chem. 126 (52) (2014) 14696–14699.

[26] C.-F. Leung, et al., A cobalt (II) quaterpyridine complex as a visible light-driven catalyst for both water oxidation and reduction, Energy Environ. Sci. 5 (7) (2012) 7903–7907.

[27] F.W.J. Teale, Cleavage of the haem-protein link by acid methylethylketone, Biochim. Biophys. Acta 35 (1959) 543.

[28] E.E. Di Iorio, [4] Preparation of derivatives of ferrous and ferric hemoglobin, in: Methods in Enzymology, vol. 76, Elsevier, 1981, pp. 57–72.

[29] N. Izadi, et al., Purification and characterization of an extracellular heme-binding protein, HasA, involved in heme iron acquisition, Biochemistry 36 (23) (1997) 7050–7057.

[30] C.L. Ladner, J. Yang, R.J. Turner, R.A. Edwards, Visible fluorescent detection of proteins in polyacrylamide gels without staining, Anal. Biochem. 326 (1) (2004) 13–20.

[31] A.G. Ferroge, M.J. Seddon, J. Skilling, N. Ordsmith, The application of 'MaxEnt' to high resolution mass spectrometry, Rapid Commun. Mass Spectrom. 6 (12) (1992) 765–770.

[32] E. Buncel, E.A. Symons, The inherent instability of dimethylformamide–water systems containing hydroxide ion, J. Chem. Soc. D Chem. Commun. (3) (1970) 164–165.

[33] Q. Yang, M. Sheng, Y. Huang, Potential safety hazards associated with using N, N-dimethylformamide in chemical reactions, Org. Process Res. Dev. 24 (9) (2020) 1586–1601.

[34] A.Y.S. Malkhasian, M.E. Finch, B. Nikolovski, A. Menon, B.E. Kucera, F.A. Chavez, N, N '-Dimethylformamide-Derived products from catalytic oxidation of 3-hydroxyflavone, Inorg. Chem. 46 (8) (2007) 2950–2952.

[35] T.R.M. Barends, et al., Direct observation of ultrafast collective motions in CO myoglobin upon ligand dissociation, Science (80-.) 350 (6259) (2015) 445–450.

[36] D.S. Culbertson, J.S. Olson, Role of heme in the unfolding and assembly of myoglobin, Biochemistry 49 (29) (2010) 6052–6063.

[37] T.E. Carver, et al., A novel site-directed mutant of myoglobin with an unusually high O2 affinity and low autooxidation rate, J. Biol. Chem. 267 (20) (1992) 14443–14450, https://doi.org/10.1016/S0021-9258(19)49732-9.

[38] W. Pfeil, Thermodynamics of apocytochrome b5 unfolding, Protein Sci. 2 (9) (1993) 1497–1501.

[39] M.J. Cocco, J.T.J. Lecomte, The native state of apomyoglobin described by proton NMR spectroscopy: interaction with the paramagnetic probe HyTEMPO and the fluorescent dye ANS, Protein Sci. 3 (2) (1994) 267–281.

[40] J.T.J. Lecomte, Y. Kao, M.J. Cocco, The native state of apomyoglobin described by proton NMR spectroscopy: the A-B-G-H interface of wild-type sperm whale apomyoglobin, Proteins: Struct., Funct., Bioinf. 25 (3) (1996) 267–285.

[41] A.Y. Alontaga, et al., Structural characterization of the hemophore HasAp from Pseudomonas aeruginosa: NMR spectroscopy reveals Protein−Protein interactions between holo-HasAp and hemoglobin, Biochemistry 48 (1) (Jan. 2009) 96–109, https://doi.org/10.1021/bi801860g.

[42] E. Blanco, J.M. Ruso, J. Sabín, G. Prieto, F. Sarmiento, Thermalstability of lysozyme and myoglobin in the presence of anionic surfactants, J. Therm. Anal. Calorim. 87 (1) (2007) 211–215, https://doi.org/10.1007/s10973-006-7842-5.

[43] Q. Zhang, C. Cao, Z. Wang, Y. Wang, H. Wu, Z. Huang, The comparative study on the solution structures of the oxidized bovine microsomal cytochrome b5 and mutant V45H, Protein Sci. 13 (8) (2004) 2161–2169.

[44] G. Centola, et al., Gallium (III)–Salophen as a dual inhibitor of Pseudomonas aeruginosa heme sensing and iron acquisition, ACS Infect. Dis. 6 (8) (2020) 2073–2085.